Letter

Interplay between jamming and motility-induced phase separation in persistent self-propelling particles

Jing Yang [1], Ran Ni [2], and Massimo Pica Ciamarra [1,3,4,*]

[1] *Division of Physics and Applied Physics, School of Physical and Mathematical Sciences, Nanyang Technological University, Singapore 637371*

[2] *Chemical Engineering, School of Chemical and Biomedical Engineering, Nanyang Technological University, Singapore 637459*

[3] *CNRS@CREATE LTD, 1 Create Way, 08-01 CREATE Tower, Singapore 138602*

[4] *CNR–SPIN, Dipartimento di Scienze Fisiche, Università di Napoli Federico II, I-80126 Napoli, Italy*

(Received 8 March 2022; accepted 31 May 2022; published 5 July 2022)

In living and engineered systems of active particles, self-propulsion induces an unjamming transition from a solid to a fluid phase and phase separation between a gas and a liquidlike phase. We demonstrate an interplay between these two nonequilibrium transitions in systems of persistent active particles. The coexistence and jamming lines in the activity-density plane meet at the jamming transition point in the limit of hard particles or zero activity. This interplay induces an anomalous dynamic in the liquid phase and hysteresis at the active jamming transition.

DOI: 10.1103/PhysRevE.106.L012601

Giant density fluctuations and collective phenomena reminiscent of equilibrium phase transitions such as flocking [1], motility-induced phase separation (MIPS) [2–5], and active crystallization [6] characterize living and engineered systems of particles able to self-propel. These phenomena emerge on increasing the strength of the self-propelling forces at the expense of other collective phenomena. For instance, in the prototypical hard-disk system, active forces affect equilibrium melting by first suppressing the liquid-hexatic coexistence and then inducing a MIPS between a low-density gaslike phase and a higher-density liquid, hexatic, or crystalline phase [7–9]. In three dimensions, the motility-induced. gas-liquid transition occurs within the gas-crystal MIPS coexistence region [10].

Active forces influence the glass and jamming transitions in systems that do not crystallize due to structural or energetic disorder, including cell aggregates [11–19], bacteria colonies [20–22], and polydisperse active Brownian particles [11,23–25]. The interplay between MIPS and jamming depends on the persistence time of the active force, which influences MIPS [26]. In two-dimensional systems of soft, bidisperse active Brownian disks [11,27] with a "small" persistence time, jamming and MIPS appear unrelated as occurring in different regions of the density or activity plane. Recent works [25,28] have investigated the limit of high persistence in models differing in polydispersity, thermal noise, and active velocity dynamics, reporting contrasting results. In [25], MIPS and jamming (glass) stay separate in the limit of high persistence, while in [28], they approach each other. While MIPS are jamming appears related in the limit of persistent particles [29], their connection and the influence of their interplay on the dynamical features has not been ascertained.

In this Letter, we demonstrate an interplay between MIPS and jamming in a two-dimensional system of active, purely repulsive particles. We focus on the limit of persistent particles [30–32] and investigate MIPS and jamming as the active forces, density, and stiffness of the particles vary. We find that the high-density gas-liquid MIPS coexistence curve and the jamming line are separated by a small volume fraction range of the liquid phase that vanishes in the limits of small activities or hard particles. In these limits, MIPS and jamming occur together. In the liquid phase, particle motion is correlated over the whole system for a long, size-dependent transient, during which particles do not preferentially move along the direction of their self-propelling force. Correlations in the direction of the active forces that build up in the liquid phase induce hysteresis at the jamming transition.

We simulate an A:B 65 : 35 binary mixture [33] of $N = 16\,000$ particles of unit mass m and diameters $d_{\rm AA}$ and $d_{\rm BB} = d_{\rm AA}/1.4$, interacting via a Lennard-Jones (LJ)-like n-m potential with $m = n/2$,

$$V_{\rm n,m}(r) = \frac{\epsilon_{\alpha\beta}}{n-m}\left[m\left(\frac{d_{\alpha\beta}}{r}\right)^{\rm n} - n\left(\frac{d_{\alpha\beta}}{r}\right)^{\rm m}\right], \qquad (1)$$

truncated in its minimum $d_{\alpha\beta}$. Hence, the interaction is purely repulsive. We fix $\epsilon_{\rm AA} = 1$, $\epsilon_{\rm BB} = 0.5\epsilon_{\rm AA}$, and $\epsilon_{\rm AB} = 1.5\epsilon_{\rm AA}$, and set $d_{AB} = 1/2(d_{\rm AA} + d_{\rm BB})$ and $n = 12$ if not otherwise stated. The area fraction is $\phi = NL^{-2}\langle a\rangle$, with $\langle a\rangle$ the average particle area [34] and L the linear size of our square simulation domain. The equation of motion for particle i is

$$m\ddot{\mathbf{r}}_i = \sum_j \boldsymbol{f}_{ij} - \gamma\dot{\mathbf{r}}_i + \mathbf{F}_{A,i}, \qquad (2)$$

where $\boldsymbol{f}_{ij}$ is the interaction force between particles i and j, $\gamma = 1$ is a damping parameter, and $\mathbf{F}_{A,i} = F_A\mathbf{e}_i$ is the self-propelling force acting on the particle. In the range of

*massimo@ntu.edu.sg

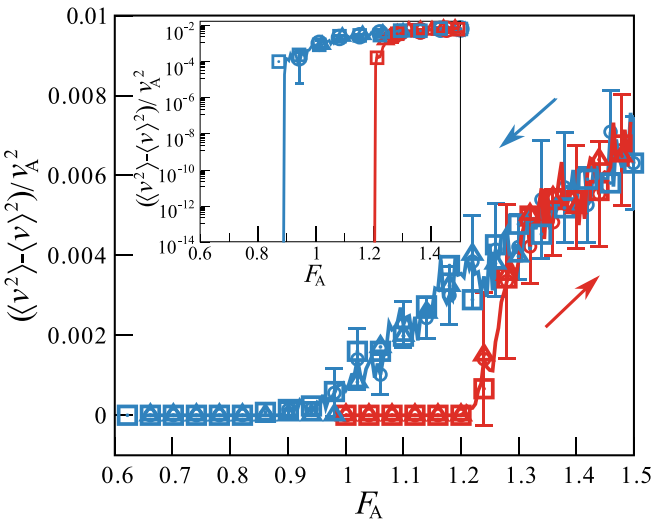

FIG. 1. Dependence of the velocity fluctuations on the active force as this decreases (blue) or increases (red) at force rates $|dF_A/dt| = 10^{-6}$ (circles), 5×10^{-7} (triangles), 2×10^{-6} (squares). The volume fraction is $\phi = 0.98$ and the stiffness exponent is $n = 12$. The abrupt variation of the kinetic energy upon jamming or unjamming illustrated in the inset allows for the unambiguous identification of the active force values of the jamming and unjamming transitions.

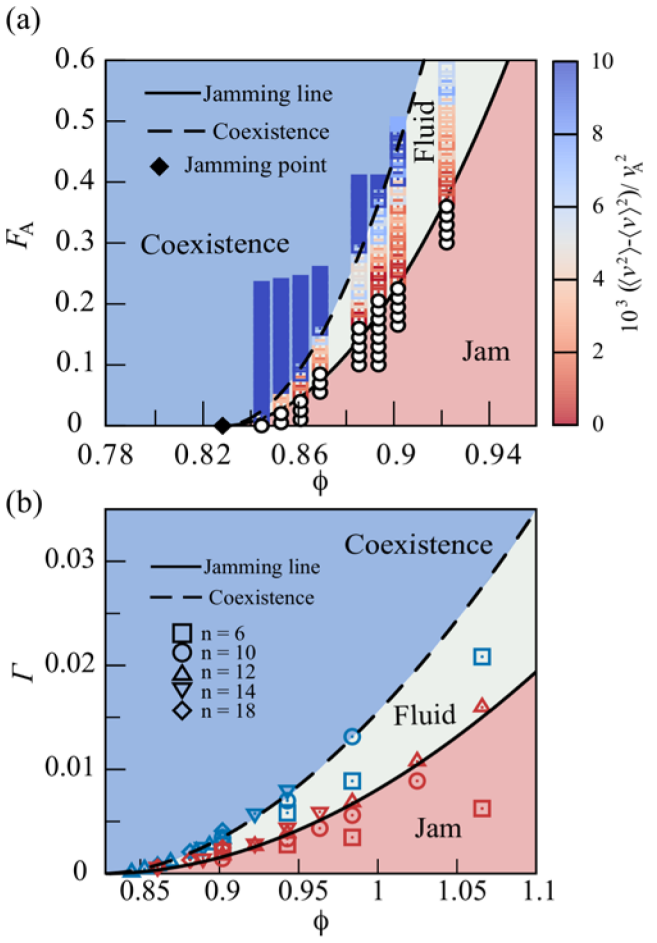

FIG. 2. (a) Phase diagram for stiffness exponent $n = 12$. Squares identifying phase-separated (full) and homogeneous (empty) states are colored according to the value of a scaled kinetic energy. White circles identify jammed configurations, and the black diamond marks the jamming volume fraction, ϕ_J. The jamming transition and the high-density branch of the coexistence line scales as $(\phi - \phi_J)^2$. The MIPS low-density branch (not shown) is at $\phi \simeq 0.2$ and depends weakly on F_A. (b) Points on the coexistence (blue) and jamming (red) lines for potentials differing in their stiffness exponent n, in the relative compression area fraction phase diagram. The coexistence (dashed) and jamming (full) lines refer to $n = 12$ as in (a).

parameters that we consider, the damping parameter γ is large enough for the inertial effect to be negligible, as we will explicitly demonstrate.

The active forces have magnitude F_A and fixed random orientations $\mathbf{e}_i$, which we chose with the constraint $\sum \mathbf{e}_i = 0$ to avoid the motion of the center of mass. We indicate with $v_A = F_A/\gamma$ and $\tau_A = d_{AA}/v_A$ the typical velocity and timescale set by the active force dynamics and particle size.

Zero-activity jamming transition. Our model reproduces the jamming phenomenology in the absence of active forces: energy minimal configurations acquire mechanical rigidity above a jamming area fraction that depends on their preparation protocol [35,36]. We investigate the jamming transition by minimizing the energy of random configurations of area fraction ϕ via the conjugate-gradient method [37], using a protocol that is not affected by inertia as our active particle simulations. We estimate the jamming volume fraction (not shown) to be $\phi_J \simeq 0.828$.

Interplay between MIPS and jamming. In the presence of active forces, the system transitions from a flowing to a jammed regime as the density increases or the magnitude of the active forces decreases. We locate this transition by determining the state point $(\phi, F_A)_J$ at which the kinetic energy of the system vanishes as F_A slowly decreases at a constant ϕ, as illustrated in Fig. 1. We repeat this study four times at each considered ϕ to estimate the average active force at jamming.

Besides controlling the jamming transition, active forces also induce MIPS between a gas and a liquidlike phase. Here, we cannot determine the MIPS phase boundary via the study of the equation of state as the pressure is not well defined for persistent self-propelling particles [38]. Henceforth, we assess phase separation by investigating the distribution of the local volume fraction ϕ_l obtained by coarse graining the system on a square grid with edge length $4\sigma_{AA}$. We summarize the result of this standard investigation [8,26,39] in the Supplemental Material (SM) [40].

The investigation of the jamming transition and the motility-induced phase separation leads to the F_A–ϕ phase diagram of Fig. 2(a). The jamming line $F_J(\phi)$ separating the fluid and the jammed phase and the high-density branch of the coexistence line, $F_C(\phi) \geqslant F_J(\phi)$, are well described by power-law functional forms vanishing at the jamming volume fraction ϕ_J, $F_J = A_J(\phi - \phi_J)^{\beta_J}$, and $F_C = A_C(\phi - \phi_J)^{\beta_C}$. We find $A_J < A_C$ and $\beta_J \simeq \beta_C \simeq 2$.

This phase diagram suggests that the coexisting phases are always of gas and a liquid type, rather than of gas and a jam type [23]. Indeed, in the coexistence region, we find that the high-density clusters have a finite lifetime, as we discuss in the SM [40].

To assess the role of the particles' stiffness, we determine the activity-volume fraction phase diagram for interaction potentials differing in their stiffness exponent n. We identify the jamming density as that at which the kinetic energy drops to zero as the active force slowly decreases in magnitude, and the coexistence density as the highest density at which the local volume fraction distribution is unimodal, at the considered F_A value. To compare these potentials, we evaluate the relative particle deformation induced by the active forces, which in the harmonic approximation is $\Gamma \propto \frac{F_A d}{\epsilon n^2}$. In the limit of small Γ, the harmonic approximation holds, and the coexistence and jamming curve of potentials with different stiffness collapse in the Γ-ϕ plane, as shown in Fig. 2(b). As Γ increases, the harmonic approximation breaks down, leading to an increase of the volume fraction range where the liquid phase occurs as the potential softens (n decreases).

Our investigation demonstrates that for persistent particles, the fluid phase vanishes at the jamming point in the $F_A \to 0$ limit or, equivalently, in the limit of hard spheres, $n \to \infty$. In these limits, MIPS and jamming meet at the jamming transition point. To explain this result, we consider in the high-density coexistence region our system appears as a dense liquid punctuated by empty cavities (see Fig. S1 in the SM [40]), as previously observed [41,42]. The shrinking of these cavities with the active force's magnitude drives the convergence of the high-density coexistence curve to the jamming point.

The convergence of jamming and MIPS has significant consequences for the speculated analogy [31,43,44] between sheared amorphous solids and dense active matter. While both the increase of shear stress and activity induces an unjamming transition, the unjammed phase is homogeneous in the case of shear forces, while it is phase separated in the limit of small persistent active forces. Furthermore, in the case of shear [45], the jamming transition line scales linearly with the overcompression $\phi - \phi_J$, in the harmonic regime, while we find it here to scale quadratically.

Anomalous dynamics in the liquid phase. The fluid phase enclosed between the coexistence and the jamming line exhibits anomalous dynamical features, which we highlight by decomposing a particle' displacement in components parallel and orthogonal to its active force, $\mathbf{\Delta} r_i = \Delta r_i \mathbf{u}_i = \Delta r_{i,n} \mathbf{e}_i + \Delta r_{i,o} \mathbf{o}_i$. This decomposition allows us to investigate the parallel $\langle \Delta r^2_{i,n}(t) \rangle$ and $\langle \Delta r^2_{i,o}(t) \rangle$ orthogonal mean square displacements (MSD). In the gas phase, the parallel MSD reflects ballistic dynamics with an effective volume fraction dependent velocity, while the orthogonal MSD reveals diffusive dynamics induced by the interparticle collisions [26], as we illustrate in Fig. 3(a).

Surprisingly, in the high-density liquid phase, parallel and orthogonal dynamics are ballistic and identical for a long transient. During this transient, displacements are not aligned to the self-propelling forces and $\langle \mathbf{u}_i \cdot \mathbf{e}_i \rangle < 1$, as shown in the bottom of Fig. 3(a). The orthogonal MSD transitions to a diffusive regime only after reaching order L^2, as we verified via a finite-size investigation (not shown). These results originate from the transient organization of the flow pattern in large structures with a size comparable to that of the system, as in Figs. 3(b)–3(d). These structures are not the turbulentlike vortices of other active matter systems [46], as their dimension is

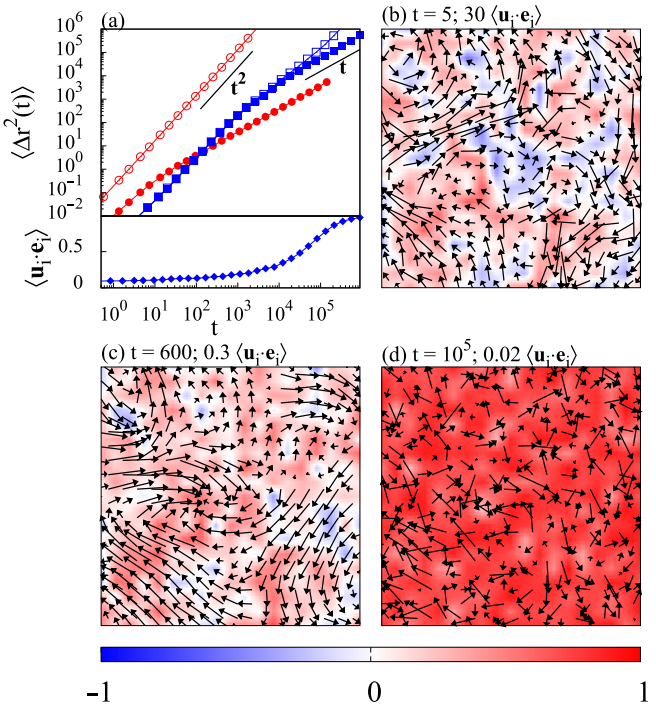

FIG. 3. (a) Top: Mean square displacement parallel (open symbols) and orthogonal (full symbols) to the self-propelling direction, in the gas (red, $\phi = 0.08$, $F_A = 0.5$) and the liquid (blue, $\phi = 0.9$, $F_A = 0.5$) phase, for a $N = 4000$ particle systems. Bottom: In the liquid phase, displacements align to the self-propelling forces after a long transient. (b)–(d) Coarse-grained displacement field in the liquid phase, at increasing times, scaled as indicated.

fixed by the system size rather than by motility and interaction parameters.

Jamming vs unjamming. A liquid configuration jams as the magnitude of the active forces becomes smaller than a threshold. Similarly, a jammed configuration starts flowing if the magnitude of randomly oriented active forces overcomes an unjamming threshold. Surprisingly, the unjamming threshold is larger than the jamming one, as apparent in Fig. 1. The difference between these two thresholds decreases with the volume fraction and vanishes at the jamming point, where the jamming and unjamming lines meet, as illustrated in Fig. 4(a). While this distinction between jamming and unjamming resembles the inertia-induced hysteresis occurring in sheared granular media [45], inertia in our system is negligible. Henceforth, the observed distinction implies differences in the configurations on the jamming and unjamming lines, which we unveil by investigating the features of their force network.

We find that configurations on the jamming and unjamming line have the same interparticle forces distribution, once the forces are scaled by their average magnitude, as we illustrate in Fig. 4(b). Active forces do not influence the force distribution as their value on the jamming and unjamming lines is a small fraction ($\simeq 1/10$) of the typical interparticle force. We investigate correlations in the interparticle forces by considering that each force $\boldsymbol{f}$ act at the contact point $\mathbf{r}_c$ of our extended interacting particles. We then study the correlation function between interaction forces at a distance

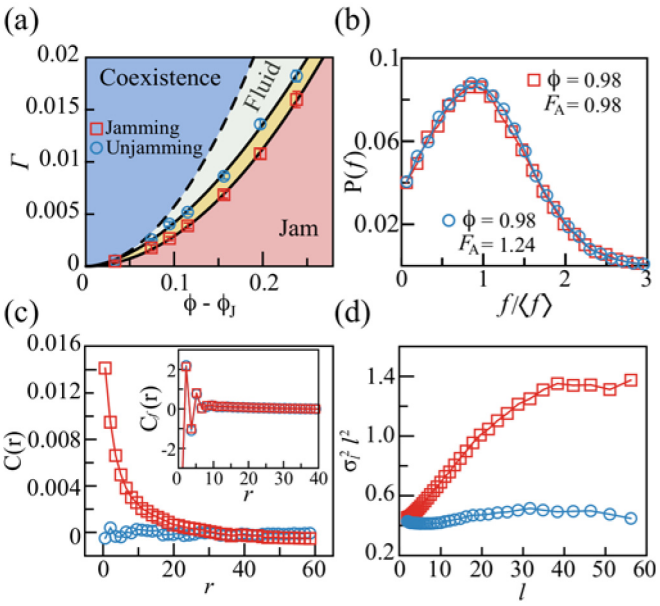

FIG. 4. (a) The jamming phase diagram of Fig. 2 ($n = 12$) with the addition of the unjamming line. The system could flow or be jammed in the yellow shaded region, depending on the preparation protocol. (b) Probability distribution of the interparticle forces on representative state points on the jamming (red squares) and on the unjamming (blue circles) line. (c) Correlation function of the interparticle force (inset) and of the self-propelling forces (main panel). (d) Scaled fluctuations $\sigma^2 l^2$ of the sum of the magnitude of the active forces found in square regions of linear size l.

$r = |\mathbf{r}_c - \mathbf{r}'_c|$, $C_f(r) = \langle |\boldsymbol{f}(\mathbf{r}_c)|^q |\boldsymbol{f}(\mathbf{r}'_c)|^q \cos(2\theta) \rangle$, where θ is the angle between the two forces and q is a parameter used to weight the contribution of forces of different magnitude to the correlation function. The factor of 2 in the cosine accounts for the fact that a contact force $\boldsymbol{f}(\mathbf{r})$ is defined up to a sign, as it could act on one of the two interacting particles. For $q = 0$, $C_f(r)$ reduces to the two-dimensional nematic correlation function. The inset of Fig. 4(c) reveals that $C_f(r)$ for $q = 1$ is the same on the jamming and unjamming lines. Analogous results occur at different q values, proving the absence of two-body correlations between the interaction forces.

We rationalize the difference between configurations on the jamming and unjamming lines considering that spatial correlations between the active forces build up in the liquid phase [28,41]. If these correlations persist as the system jams, then they induce correlations in the interparticle forces as in a jammed configuration $\mathbf{F}_{A,i} = -\sum_j \boldsymbol{f}_{ij}$. We check this possibility by investigating the correlation function of the active force direction, $C(r) = \langle \mathbf{e}_i(0) \cdot \mathbf{e}_j(r) \rangle$, in Fig. 4(c). At the unjamming threshold, forces are uncorrelated, so that $C(r) = 0$. Conversely, on the jamming line, $C(r)$ only approaches zero at large distances. As an alternative measure of correlations of the interparticle forces, we investigate the fluctuations σ_l^2 of $|\sum_{i \in l^2} \mathbf{F}_{A,i}|$, where the sum is over all particles located in square regions of linear size l. At the unjamming threshold, forces are uncorrelated, and in Fig. 2(d), we find $\sigma_l^2 \propto l^2$ at all l, as dictated by the central limit theorem. Conversely, on the jamming line, the above scaling signaling the absence of correlations only occurs for large l. The results of Figs. 2(b) and 2(d) consistently show the existence of many-body [47] correlations extending up to $r \simeq 30$ in the considered configuration. We have not observed clear variations of this correlation length along the jamming line. Henceforth, while forces on the unjamming line are uncorrelated, those on the jamming line possess many-body correlations.

Discussion. Our results demonstrate an interplay between jamming and motility-induced phase separation in systems of persistent self-propelling particles. In the Γ-ϕ plane, with Γ a measure of the relative particle deformation induced by the active force, the MIPS and jamming lines meet in the $\Gamma \to 0$ limit (hard sphere or zero activity) at the jamming point. This interplay induces surprising size effects in the dynamics of the liquid phase separating MIPS and jamming at finite Γ. Particle motion is collective on a length comparable to that of the system for a long transient also scaling with the system size. During this transient, particle displacements do not correlate with the directions of the self-propelling forces. In this liquid phase, active forces develop spatial correlations that persist as the system jams, inducing many-body correlations in the interparticle forces of jammed configurations. In the presence of a finite and large persistent time, at high density the system evolves through an intermittent avalanche dynamics [23]. The huge many-body correlations in the interparticle forces we have reported may explain why these avalanches are extensive.

Acknowledgments. We acknowledge support from the Singapore Ministry of Education through the Singapore Academic Research Fund, Grants No. RG86/19 and No. RG56/21, and the National Supercomputing Centre Singapore (NSCC) for the computational resources.

[1] T. Vicsek, A. Czirók, E. Ben-Jacob, I. Cohen, and O. Shochet, Novel Type of Phase Transition in a System of Self-Driven Particles, Phys. Rev. Lett. **75**, 1226 (1995).

[2] Y. Fily and M. C. Marchetti, Athermal Phase Separation of Self-Propelled Particles with No Alignment, Phys. Rev. Lett. **108**, 235702 (2012).

[3] M. C. Marchetti, J. F. Joanny, S. Ramaswamy, T. B. Liverpool, J. Prost, M. Rao, and R. A. Simha, Hydrodynamics of soft active matter, Rev. Mod. Phys. **85**, 1143 (2013).

[4] C. Bechinger, R. Di Leonardo, H. Löwen, C. Reichhardt, G. Volpe, and G. Volpe, Active particles in complex and crowded environments, Rev. Mod. Phys. **88**, 045006 (2016).

[5] M. E. Cates and J. Tailleur, Motility-induced phase separation, Annu. Rev. Condens. Matter Phys. **6**, 219 (2015).

[6] J. Palacci, S. Sacanna, A. P. Steinberg, D. J. Pine, and P. M. Chaikin, Living crystals of light-activated colloidal surfers, Science **339**, 936 (2013).

[7] J. Bialké, T. Speck, and H. Löwen, Crystallization in a Dense Suspension of Self-Propelled Particles, Phys. Rev. Lett. **108**, 168301 (2012).

[8] G. S. Redner, M. F. Hagan, and A. Baskaran, Structure and Dynamics of a Phase-Separating Active Colloidal Fluid, Phys. Rev. Lett. **110**, 055701 (2013).

[9] P. Digregorio, D. Levis, A. Suma, L. F. Cugliandolo, G. Gonnella, and I. Pagonabarraga, Full Phase Diagram of Active Brownian Disks: From Melting to Motility-Induced Phase Separation, Phys. Rev. Lett. **121**, 098003 (2018).

[10] A. K. Omar, K. Klymko, T. GrandPre, and P. L. Geissler, Phase Diagram of Active Brownian Spheres: Crystallization and the Metastability of Motility-Induced Phase Separation, Phys. Rev. Lett. **126**, 188002 (2021).

[11] S. Henkes, Y. Fily, and M. C. Marchetti, Active jamming: Self-propelled soft particles at high density, Phys. Rev. E **84**, 040301(R) (2011).

[12] S. Henkes, K. Kostanjevec, J. M. Collinson, R. Sknepnek, and E. Bertin, Dense active matter model of motion patterns in confluent cell monolayers, Nat. Commun. **11**, 1405 (2020).

[13] D. Bi, X. Yang, M. C. Marchetti, and M. L. Manning, Motility-Driven Glass and Jamming Transitions in Biological Tissues, Phys. Rev. X **6**, 021011 (2016).

[14] S. Garcia, E. Hannezo, J. Elgeti, J.-F. Joanny, P. Silberzan, and N. S. Gov, Physics of active jamming during collective cellular motion in a monolayer, Proc. Natl. Acad. Sci. **112**, 15314 (2015).

[15] F. Giavazzi, M. Paoluzzi, M. Macchi, D. Bi, G. Scita, M. L. Manning, R. Cerbino, and M. C. Marchetti, Flocking transitions in confluent tissues, Soft Matter **14**, 3471 (2018).

[16] A. Mongera, P. Rowghanian, H. J. Gustafson, E. Shelton, D. A. Kealhofer, E. K. Carn, F. Serwane, A. A. Lucio, J. Giammona, and O. Campàs, A fluid-to-solid jamming transition underlies vertebrate body axis elongation, Nature (London) **561**, 401 (2018).

[17] A. Pasupalak, L. Yan-Wei, R. Ni, and M. Pica Ciamarra, Hexatic phase in a model of active biological tissues, Soft Matter **16**, 3914 (2020).

[18] Y.-W. Li, L. L. Y. Wei, M. Paoluzzi, and M. P. Ciamarra, Softness, anomalous dynamics, and fractal-like energy landscape in model cell tissues, Phys. Rev. E **103**, 022607 (2021).

[19] E. Lawson-Keister and M. L. Manning, Jamming and arrest of cell motion in biological tissues, Curr. Opin. Cell Biol. **72**, 146 (2021).

[20] B. R. Parry, I. V. Surovtsev, M. T. Cabeen, C. S. O'Hern, E. R. Dufresne, and C. Jacobs-Wagner, The bacterial cytoplasm has glass-like properties and is fluidized by metabolic activity, Cell **156**, 183 (2014).

[21] M. Delarue, J. Hartung, C. F. Schreck, P. Gniewek, L. Hu, S. Herminghaus, and O. Hallatschek, Self-driven jamming in growing microbial populations, Nat. Phys. **12**, 762 (2016).

[22] J. Yang, P. E. Arratia, A. E. Patteson, and A. Gopinath, Quenching active swarms: Effects of light exposure on collective motility in swarming serratia marcescens, J. R. Soc. Interface **16**, 20180960 (2019).

[23] R. Mandal, P. J. Bhuyan, P. Chaudhuri, C. Dasgupta, and M. Rao, Extreme active matter at high densities, Nat. Commun. **11**, 2581 (2020).

[24] R. Mandal and P. Sollich, Multiple Types of Aging in Active Glasses, Phys. Rev. Lett. **125**, 218001 (2020).

[25] M. Paoluzzi, D. Levis, and I. Pagonabarraga, From motility-induced phase-separation to glassiness in dense active matter, Commun. Phys. **5**, 111 (2022).

[26] P. Nie, J. Chattoraj, A. Piscitelli, P. Doyle, R. Ni, and M. P. Ciamarra, Stability phase diagram of active brownian particles, Phys. Rev. Research **2**, 023010 (2020).

[27] Y. Fily, S. Henkes, and M. C. Marchetti, Freezing and phase separation of self-propelled disks, Soft Matter **10**, 2132 (2014).

[28] Y.-E. Keta, R. L. Jack, and L. Berthier, Disordered collective motion in dense assemblies of persistent particles, arXiv:2201.04902.

[29] C. Villarroel and G. Düring, Critical yielding rheology: from externally deformed glasses to active systems, Soft Matter **17**, 9944 (2021).

[30] C. Merrigan, K. Ramola, R. Chatterjee, N. Segall, Y. Shokef, and B. Chakraborty, Arrested states in persistent active matter: Gelation without attraction, Phys. Rev. Research **2**, 013260 (2020).

[31] Q. Liao and N. Xu, Criticality of the zero-temperature jamming transition probed by self-propelled particles, Soft Matter **14**, 853 (2018).

[32] C. Reichhardt and C. J. Olson Reichhardt, Absorbing phase transitions and dynamic freezing in running active matter systems, Soft Matter **10**, 7502 (2014).

[33] R. Brüning, D. A. St-Onge, S. Patterson, and W. Kob, Glass transitions in one-, two-, three-, and four-dimensional binary Lennard-Jones systems, J. Phys.: Condens. Matter **21**, 035117 (2009).

[34] $\langle a \rangle = \frac{\pi}{4}[0.64 d_{\mathrm{AA}}^2 + 0.35 d_{\mathrm{BB}}^2])$.

[35] P. Chaudhuri, L. Berthier, and S. Sastry, Jamming Transitions in Amorphous Packings of Frictionless Spheres Occur over a Continuous Range of Volume Fractions, Phys. Rev. Lett. **104**, 165701 (2010).

[36] M. Pica Ciamarra, A. Coniglio, and A. De Candia, Disordered jammed packings of frictionless spheres, Soft Matter **6**, 2975 (2010).

[37] C. S. O'Hern, S. A. Langer, A. J. Liu, and S. R. Nagel, Random Packings of Frictionless Particles, Phys. Rev. Lett. **88**, 075507 (2002).

[38] A. P. Solon, Y. Fily, A. Baskaran, M. E. Cates, Y. Kafri, M. Kardar, and J. Tailleur, Pressure is not a state function for generic active fluids, Nat. Phys. **11**, 673 (2015).

[39] T. Speck, J. Bialké, A. M. Menzel, and H. Löwen, Effective Cahn-Hilliard Equation for the Phase Separation of Active Brownian Particles, Phys. Rev. Lett. **112**, 218304 (2014).

[40] See Supplemental Material at http://link.aps.org/supplemental/10.1103/PhysRevE.106.L012601 for additional information.

[41] A. Wysocki, R. G. Winkler, and G. Gompper, Cooperative motion of active Brownian spheres in three-dimensional dense suspensions, Europhys. Lett. **105**, 48004 (2014).

[42] J. Bialké, J. T. Siebert, H. Löwen, and T. Speck, Negative Interfacial Tension in Phase-Separated Active Brownian Particles, Phys. Rev. Lett. **115**, 098301 (2015).

[43] L. Berthier, Nonequilibrium Glassy Dynamics of Self-Propelled Hard Disks, Phys. Rev. Lett. **112**, 220602 (2014).

[44] P. K. Morse, S. Roy, E. Agoritsas, E. Stanifer, E. I. Corwin, and M. L. Manning, A direct link between active matter and sheared granular systems, Proc. Natl. Acad. Sci. USA **118**, e2019909118 (2021).

[45] M. Pica Ciamarra and A. Coniglio, Jamming at Zero Temperature, Zero Friction, and Finite Applied Shear Stress, Phys. Rev. Lett. **103**, 235701 (2009).

[46] R. Alert, J. Casademunt, and J.-F. Joanny, Active turbulence, Annu. Rev. Condens. Matter Phys. **13**, 143 (2022).

[47] Y. Zheng, A. D. S. Parmar, and M. Pica Ciamarra, Hidden Order Beyond Hyperuniformity in Critical Absorbing States, Phys. Rev. Lett. **126**, 118003 (2021).